Optics and Photonics Journal, 2026, 16(1), 1-11
https://www.scirp.org/journal/opj
ISSN Online: 2160-889X
ISSN Print: 2160-8881

One-Way Interferometer for Implementing the Generalized Sagnac Effect

V. K. Sakharov

JSC "Center VOSPI", Moscow, Russia
Email: vk_sach@mail.ru

How to cite this paper: Sakharov, V.K. (2026) One-Way Interferometer for Implementing the Generalized Sagnac Effect. *Optics and Photonics Journal*, **16**, 1-11.
https://doi.org/10.4236/opj.2026.161001

Received: January 2, 2026
Accepted: January 28, 2026
Published: January 31, 2026

Abstract

This article discusses a hypothetical device—the one-way interferometer based on the generalized Sagnac effect for studying rotational and uniform rectilinear motion. The key element of this device is an electro-optical deflector installed in one arm of a two-beam interferometer for scanning the traveling wave over a limited range of angles. When interfering with the reference wave, this will lead to oscillations in the light-driven photocurrent at the device output and will allow, when processing the photocurrent, to extract at the fundamental frequency of oscillations the phase shift of one (scanning) wave with information about the speed of movement, arising as a result of the generalized Sagnac effect. The stability of the interference will be ensured by the selected scanning amplitude and feedback of the frequency component at double the scanning frequency with the phase of the reference wave. If confirmed experimentally, the one-way interferometer will provide greater insight into the nature of the generalized Sagnac effect and identify potential applications in scientific and applied research. To test the performance of the one-way interferometer, an experiment is being considered to measure the orbital velocity of the Earth around the Sun and, together with the Solar System, around the center of the Galaxy, as well as the speed of the Earth's translational motion relative to the Cosmic Microwave Background.

Keywords

Generalized Sagnac Effect, One-Way Interferometer, Phase Shift, Rotational and Uniform Rectilinear Motion

1. Introduction

It was generally believed that the Sagnac effect occurs when counterpropagating optical waves travel along a rotating closed loop. However, R. Wang, Y. Zheng, A.

Yao, and D. Langley discovered that a similar effect also occurs during uniform rectilinear motion of a closed loop [1] [2]. The authors used a device in the form of a closed fiber-optic circuit, consisting of linearly and circularly moving sections through which counterpropagating waves propagated. The emitter-receiver module moved along with the moving optic fiber, used to transmit and receive counterpropagating waves and also to determine the phase difference of these waves.

It has been shown that any section of a fiber optic conveyor, regardless of the refractive index of the fiber and the nature of the motion, whether it be rectilinear motion or rotation, makes a contribution to the total phase difference of the counterpropagating waves, proportional to the product of the length of the segment l, the linear speed of its movement V relative to the fixed base of the conveyor, and the cosine of the angle φ between the directions of light propagation in the segment and the direction of its movement:

$$\Delta\Psi = 4\pi\frac{V\Delta l}{c\lambda}\cos\varphi, \tag{1}$$

where c is the speed of light in a vacuum and λ is the wavelength of light.

This effect, dubbed the generalized Sagnac effect (GSE) by the authors and including the standard Sagnac effect as a special case, is of great interest from both applied and scientific perspectives. However, this did not lead to practical use, although the authors of the effect pointed out the possible use of fiber optic conveyors in seismology as a sensor for measuring linear motion at the nanoscale.

Discussion of GSE in the literature has been limited, likely due to the fact that other applications of the fiber-optic conveyor are unlikely due to the specific nature of its design, as well as the still unknown nature of the effect. The general view of theoretical physicists [3]-[5] is that there is no definitive explanation for GSE and that further research is required, analyzing the results in the context of standard Special Relativity and its alternative variants, which assume the existence of a privileged inertial frame.

It is clear that in order to use the GSE in scientific and applied research, it is necessary to confirm this effect and develop a device that is more technologically advanced than a fiber optic conveyor and as useful as an optical gyroscope based on the Sagnac effect. Namely, such a device, which, when installed on any moving or stationary object, could react and determine the speed of this object relative to the Earth and, more importantly, the linear speed of the Earth itself, caused by its rotation, and also, possibly, the speed of its translational motion in space.

The possibility of finding such an alternative to the fiber optic conveyor is provided by the very fact of the existence of the GSE, which consists of the occurrence of a phase shift of waves running along the moving sections of the fiber optic conveyor. Measuring phase shifts of this kind underlies the operation of the optical gyroscope and is used in other navigation systems, including global positioning systems for correcting atomic clocks.

Another message for finding an alternative to fiber optic conveyor is the simple idea that if phase shift occurs when counterpropagating waves travel along a mov-

ing closed loop, it also occurs when a single wave travels along any open moving path. The problem is finding a way to measure this phase shift.

Finally, it is obvious that neither a fiber optic conveyor nor any known two-beam interferometer can respond to the rotational and linear motion of the objects on which they are placed. This is explained by the reason that in all these cases, the phase shifts of two waves, either counterpropagating or propagating in the two arms of the interferometer, resulting from the GSE are identically equal by expression (1) and therefore they mutually compensate each other when they interfere.

The sought-after alternative to the fiber-optic conveyor may be the one-way interferometer (OWI) considered in this paper, in which the measurement of the speed of movement is performed by recording the phase shift of a wave running along one of the arms of a two-beam interferometer in one direction.

This wave must be marked in some way so that when processing the photocurrent, its phase shift can be separated from the phase of the reference wave running along the other arm of the interferometer and also experiencing the effect of the GSE. Marking can be done using fast scanning the wave in a small angular range [6], while the phase shift of the scanning wave will be determined by the length of the interferometer arm L, the linear velocity of movement V and the angle between the directions of propagation of light and movement of the object $\varphi(t)$:

$$\Delta\Psi(t) = 2\pi\frac{VL}{c\lambda}\cos\varphi(t). \tag{2}$$

As shown below, the interference between the scanning and reference waves will cause oscillations in the light intensity and the photocurrent at the device output. The processing of photocurrent must be carried out by considering it as a series of harmonics with frequencies that are multiples of the scanning frequency, and by extracting two frequency components from this series: one at the fundamental frequency, *i.e.*, the scanning frequency, and one at a doubled frequency. The harmonic of the photocurrent at the fundamental frequency will be used to extract the phase shift of the scanned wave (2), which contains information about the speed of movement. The harmonic at a doubled frequency, coupled by feedback loop with the phase of the reference wave, as well as the selected scanning amplitude, will ensure interference stability.

The phase shift $\Delta\Psi(t)$ in (2) differs from the phase shift $\Delta\Psi$ in (1) in that, firstly, it is the phase shift of one wave, and not the difference between the phase shifts of two waves. Secondly, the phase shift $\Delta\Psi(t)$ is equally the result of both circular and rectilinear motion, and is determined by the vector sum of the velocities of several motions. For example, the speed of the object on which an OWI is located, plus the speeds of the Earth's daily and orbital rotation, the Earth's movement around the center of the Galaxy, and the Earth's translational motion in space, if it exists.

Thus, the purpose of this article is to present the OWI that uses electro-optical scanning of a wave in one arm of a two-beam interferometer to measure the phase

advance of the wave caused by the GSE. A possible experiment is also considered to confirm the functionality of this device and the possibility of using it to measure the speed of circular and linear motion.

2. Design and Signal Processing

The key element of the OWI is an electro-optical deflector—a device capable of changing the direction of light beams over a small range of angles using an electric field. The advantage of an electro-optical deflector over mechanical scanners is the absence of moving parts, which ensures high speed of conversion of the control signal into a scanning angle and the absence of vibrational noise, which is undesirable in interferometry.

The deflector's operation is based on the electro-optic effect. which involves modulating the refractive index of a material in response to an applied electric field. Two types of electro-optic effects are distinguished: linear and quadratic [7]. The linear electro-optic effect, known as the Pockels effect, occurs in $LiNbO_3$, $LiTaO_3$, and others crystals, where the refractive index and, consequently, the scanning angle change linearly with the electric field. If the refractive index changes quadratically with the field, this is a quadratic electro-optic effect, known as the Kerr effect.

The OWI uses an optical deflector based on the linear electro-optic effect. The scanning angles are quite small, no more than 5÷6 mrad, but due to the high sensitivity of the OWI, large scanning angles are not required. This, along with the small size of the deflector and the short length of the interferometer arms, makes the device compact, ensuring its high resistance to adverse external influences.

The OWI is mounted on a rotary support device. It provides controlled orientation of the scanning beam direction in azimuth (horizontal angle, 0˚ - 180˚) and elevation angle (vertical elevation angle, 0˚ - 90˚), as well as rotation of the platform with the interferometer around an axis parallel to the scanning plane (0˚ - 180˚).

A special feature of the optical scheme (**Figure 1**) is that the important components are taken from the element base of fiber-optic communication lines, which simplifies the equipment of the interferometer. This is a laser diode (LD), a fiber optic coupler, an electro-optic phase modulator and a photodetector. The ports of the first three components are polarization-maintaining (PM) optical fibers.

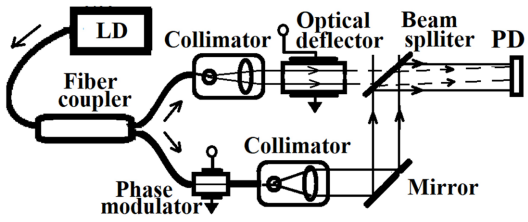

Figure 1. Optical scheme of the OWI.

The crystal of the electro-optical deflector has a diameter of $d_0 \cong 1$ mm and a

length of $l = 10$ mm. A sinusoidal electrical signal is applied to its control electrodes, causing scanning of the light passing through the deflector. The beam's deflection angle from the scanning sector axis varies according to the harmonic law $\alpha(t) = \alpha_0 \sin\omega$, where $\omega \approx 50$ kHz is the angular scanning frequency and $a_0 = 4 \div 6$ mrad is the scanning angle amplitude. The deflector is mounted such that the scanning plane of the light beam is parallel to the platform surface, and the scanning axis is orthogonal to the surface of the photodetector's input window.

A pigtail LD with PM optical fiber is used as a light source; the wavelength of its single-frequency radiation is $\lambda \approx 1.0$ μm, and its intensity is several mille watts. Using a PM fiber optical coupler, the laser beam is split into two waves with a 2:1 output power ratio. The higher-power wave is directed to a phase modulator (its insertion loss is ~3 dB), and the other wave is directed to a collimator installed in front of the optical deflector.

At the collimator input, the wave is extracted from the PM optic fiber, passes through this device, is converted into a diffraction-limited light beam with a diameter of 0.9 mm, and enters the input of the optical deflector. The deflector scans the wave, which then runs along the open path arm of the interferometer with a length of L = 5 cm and hits the input window of the photodetector.

The other wave, passing through the $LiNbO_3$ phase modulator, enters the collimator's input and is converted into a wave with a flat front with a diameter of D = 1.0 mm. Then, with the help of two mirrors—a swerve and semi-translucent mirror—this wave, which is the reference wave, is directed to the photodetector and interferes with the scanning wave.

Assuming the powers of both waves to be equal and denoting them as I_0, we write the complex amplitudes of the electric field of the interfering waves as:

$$\begin{aligned} E_1(t,V,\varphi) &= E_1 \exp\left[j\left(\varpi t + \Phi_1(t,V,\varphi)\right)\right], \\ E_2(t,V) &= E_2 \exp\left[j\left(\varpi t + \Phi_2(V,\varphi)\right)\right], \end{aligned} \tag{3}$$

where $E_1 = E_2 = \sqrt{I_0}$ —are the amplitudes of the scanning and reference waves, ϖ is the angular frequency of light, $\Phi_1(t,V,\varphi)$ and $\Phi_2(t,V,\varphi)$ are the phases of the scanning and reference waves, respectively, and φ is the angle between the direction of the velocity V and the axis of the scanning sector. In this case, we believe that the wave scanning plane is parallel to the direction of the velocity vector.

We will represent the phase of the scanned wave $\Phi_1(t,V,\varphi)$ as the sum of three phases:

$$\Phi_1(t,V,\varphi) = F_1(t) + \Psi_1(t,V,\varphi) + \tilde{\phi}_1, \tag{4}$$

where $F_1(t)$ is the phase determined by the length of the interferometer arm:

$$F_1(t) = \frac{2\pi L}{\lambda \cos\alpha(t)} \cong \frac{2\pi L}{\lambda}\left(1 + \frac{\alpha(t)^2}{2}\right) \cong \frac{2\pi L}{\lambda}\left(1 + \frac{\alpha_0^2}{4} + \frac{\alpha_0^2}{4}\cos 2\omega t\right), \tag{5}$$

$\Psi_1(t,V,\varphi)$ —the phase shift resulting from the action of GSE:

$$\Psi_1(t,V,\varphi)=\frac{2\pi LV}{\lambda\cos(\alpha)c}\left[\cos(\varphi-\alpha)\right]\cong\frac{2\pi L}{\lambda}\frac{V}{c}\left[\cos\varphi+\alpha\sin\varphi\right], \tag{6}$$

and $\tilde{\phi}_1$ is the random phase introduced by the instability of external factors.

The phase of the reference wave $\Phi_2(V,\varphi)$ is represented as the sum of four phases:

$$\Phi_2(V,\varphi)=F_2+\Psi_2(V,\varphi)+\phi_r+\tilde{\phi}_2, \tag{7}$$

where F_2 —phase determined by the length of the reference arm, $\Psi_2(V,\varphi)$ —phase shift as a result of the impact GSE, ϕ_r —phase introduced by a phase modulator and $\tilde{\phi}_2$ —random phase.

The intensity of the electric field of interfering waves is determined by the square of the modulus of the sum of the electric fields of these waves:

$$I_0(t,V,\varphi)=2I_0+2I_0\cos\Delta\Phi(t,V,\varphi), \tag{8}$$

where $\Delta\Phi(t,V,\varphi)=\Phi_1(t,V,\varphi)-\Phi_2(V,\varphi)$ —the phase difference of the two waves.

The photodetector converts the light intensity into a photocurrent and amplifies it. As a result, the signal to the photodetector's load, averaged over a short period of time and proportional to the field intensity, contains both DC and AC components. The AC component of the signal is written as

$$U_{\approx}(t,V,\varphi)=2\eta I_0\cos\Delta\Phi(t,V,\varphi), \tag{9}$$

where η is a coefficient that takes into account the sensitivity of the photodetector and its amplification using electronics.

For further calculations, we represent the phase difference $\Delta\Phi(t,V,\varphi)$ as three phase components:

$$\Delta\Phi(t,V,\varphi)=\Delta\psi\sin\omega t+y\cos 2\omega t+z, \tag{10}$$

where $\Delta\psi$ is the amplitude of the phase shift of the scanning wave as a result of GSE:

$$\Delta\psi=2\pi a_0\frac{VL}{c\lambda}\sin\varphi, \tag{11}$$

y is the amplitude of the phase component of the phase difference at frequency 2ω:

$$y=a_0^2\frac{2\pi L}{4\lambda}\left(1+\frac{V}{c}\cos\varphi\right)\cong a_0^2\frac{2\pi L}{4\lambda}, \tag{12}$$

and $z=2\pi\frac{VL\cos\varphi}{c\lambda}+\frac{2\pi L}{\lambda}\left(1+\frac{a_0^2}{4}\right)+y+\tilde{\phi}_1-\Phi_2(V,\varphi)$ —a phase which, in the absence of feedback, can have any actual value, but in its presence, it takes on and maintains a specified value.

We transform the photocurrent expression (9) using trigonometric formulas into the sum of four terms, each product of three harmonic functions whose arguments are the three phase components from (10). Using the Jacobi-Anger identities, we expand all harmonic functions into a series in Bessel functions and rep-

resent the photocurrent as a large series of harmonics with frequencies that are multiples of the scanning frequency.

In the resulting expression, we leave only two components—at the scanning frequency ω and at the doubled frequency 2ω, since only they will be extracted from the photocurrent using synchronous detection:

$$U_{\approx}(t,V,\varphi)=2\eta I_0\left[2J_1(\Delta\psi)J_0(y)\sin z\sin\omega t+2J_0(\Delta\psi)J_1(y)\sin z\cos 2\omega t\right], \quad (13)$$

where $J_n(p)$ are the Bessel functions of the first kind, n is the order, p is the argument of the functions and, as is known, the Bessel functions of the first kind are odd, *i.e.* $J_n(-x)=(-1)^n J_n(x)$.

The two components of the photocurrent (13) must each fulfill their own role. The component of the photocurrent at the scanning frequency must be used as an output signal with information on the speed of movement; the component at double the frequency must be used to create conditions that ensure the stability of the output signal and its significant level.

This requires that both Bessel functions in expression (13) have sufficiently large absolute values, and that the function $J_0(y)$ could also be adjustable to control the sensitivity of the interferometer. The required phases y can be determined using analytical expressions for these Bessel functions $J_n(y)=\sqrt{2/\pi y}\cos\left(y-\frac{n\pi}{2}-\frac{\pi}{4}\right)$ and their graphs, shown in Figure 2. It can be seen that the required condition is satisfied by phases y in the range of 1.3 ÷ 2.0 rad, the corresponding range of scanning amplitudes, according to (12), will be 4.0 ÷ 5.2 mrad, and the value of the function $J_0(y)$ can change by approximately 5 times.

Another condition for stability and a high output signal level is a phase value of $z=2\pi m+\pi/2$ (m is any integer), since in this case $\sin z=1$ and, accordingly, the level of both harmonics is sufficiently high. For this purpose, a second-harmonic feedback loop with phase z is used, where the actuator is a $LiNbO_3$ phase modulator in the reference arm, and the function of PID feedback controller is performed programmatically. The second-harmonic level also depends on the value of $J_0(\Delta\psi)$, which is certainly sufficiently high for $|\Delta\psi|\le 1$.

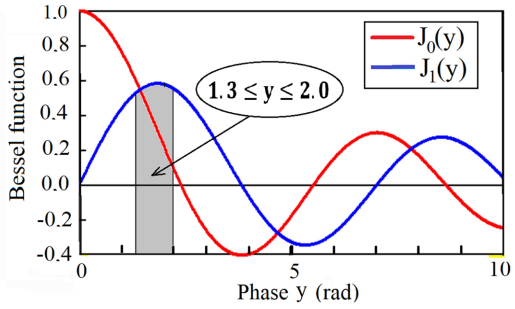

Figure 2. The graphs of Bessel functions $J_0(y)$ and $J_1(y)$.

Thus, the output signal of OWI at small phase $\Delta\psi$ is represented by the ex-

pression

$$U_{\omega}(t,V,\varphi)=2\eta I_0 J_0(y)\Delta\psi\,, \tag{14}$$

where it is taken into account that the Bessel function $J_1(x)$ for $|x|<1$ is approximated by the expression $J_1(x)\approx x/2$.

A characteristic feature of the output signal is its dependence on the angle φ between the directions of the linear velocity of movement and the scanning axis, which follows from (11)—the output signal takes on a maximum value when $\varphi=90^{\circ}$, and, conversely, drops to zero when $\varphi=0^{\circ}$. This property will allow you to determine the direction of velocity.

It is known that, when using laser radiation, modulation techniques for interferometric measurements allow one to measure periodic changes in phase difference, the lower level of which is 10^{-7} - 10^{-6} rad [8], with the main sources of interference considered to be photocurrent shot noise and thermal noise of the electronics. Since there are no fundamental differences in this respect between the interferometer under consideration and well-known interferometers used in similar measurements, the sensitivity threshold of the OWI will be at the same level.

As for technical limitations, such as ambient temperature instability, vibrations, laser noise, etc., their effect will be significantly less than in other interferometers (for example, in a fiber-optic gyroscope), since the length of the scanned wave path, where these noises can appear, is very insignificant.

The OWI calibration can be accomplished using phase modulation of the reference wave in the absence of scanning. For this purpose, two harmonic signals at frequencies ω and 2ω with amplitudes of, for example, $\Delta\psi_{\text{clb}}\approx 10^{-2}$ rad and $y_{\text{clb}}\approx 1.5$ rad are fed to the input of the phase modulator; the loop feedback of the second harmonic of the photocurrent with the control signal is preserved. The output signal in this case will be

$$U_{\omega}^{\text{clb}}(t,V,\varphi)=2\eta I_0 J_0(y_{\text{cal}})\Delta\psi_{\text{clb}}\,. \tag{15}$$

Combining (14) and (15) will allow us to determine the value of the coefficient η, which sets the sensitivity of the photodetector.

The calculation of the output signal in the OWI proves the possibility of measuring the phase shift resulting from the GSE, however, only an experiment can actually confirm the operability of this device.

3. An Experiment to Test the Functionality of the OWI

As is well known, the Michelson interferometer (MI), originally created for experiments to detect the Earth's motion relative to the ether, failed to live up to expectations in this regard, but became the basis for Special Relativity. Currently, the only type of interferometer used to study the Earth's motion, specifically its rotation around its axis, is the ring interferometer.

Relatively recently, G. Malykin and V. Pozdnyakova proposed to measure the linear velocity of the Earth's orbital motion around the Sun using the "quadratic Sagnac effect" (QSE), using a MI [9]. The calculation of this effect arising from

the rotation of the MI is based on the Sagnac effect model, considered as a result of the influence of the gravitational potential of the Coriolis force on the waves propagating in the orthogonal arms of the MI.

From the calculation it follows that the phase difference of the waves in the MI is proportional to the length of the MI arms, the square of the ratio of the linear velocity of motion $V_{\text{orbit}} \approx 30$ km·s^{-1} to the speed of light and also depends on the latitude of the measurement site and the position of the MI arms relative to the plane of the Earth's orbit, which changes during the day.

The maximum phase difference of waves $\Delta\psi_{\max}$ as a result of the influence of the MI on the waves traveling along the two arms of the IM occurs when one arm coincides with the direction of the linear velocity of the orbital motion, and the other arm is perpendicular to the first. With the length of the IM arms of 20 cm at the latitude in the central European part of Russia, the value of $\Delta\psi_{\max}$ should be 6.7×10^{-3} rad at the most favorable time of day for observing the QSE and 3.0×10^{-4} rad at the least favorable time.

The motion caused by the daily rotation of the Earth was not taken into account due to the small value of its linear velocity V_{earth}, equal to 0.5 km·s^{-1} at the equator, and the motion of the entire Solar System around the center of the Galaxy, the velocity of which is V_{Gal} ~230 km·s^{-1}, was also not taken into account. The latter was argued by the fact that such a significant linear velocity as V_{Gal} should have manifested itself as a result of the QSE effect in the well-known experiments of D. Miller on measuring the linear velocity of the Earth's motion relative to the hypothetical "luminiferous ether" [10]. However, the linear velocity V_{Gal} did not manifest itself in these experiments, a probable reason for which could have been the rotation of different subsystems of the Galaxy at different speeds, caused by the structure of the Galaxy as a complex distributed system.

Obviously, the OWI can be used in studies similar to the one proposed by the authors of the QES. With interferometer parameters $L = 5$ cm and $a_0 = 5$ mrad, the scanning axis oriented perpendicular to the direction of the Sun, and the scanning plane positioned parallel to the direction of orbital motion, the phase shift $\Delta\psi$, according to (11), should be 5.1×10^{-2} rad.

Such an experiment could also measure the velocity of the Earth's circular motion (along with the Solar System) around the galactic center. The contribution to the phase $\Delta\psi$ at a velocity of V_{Gal} ~230 km·s^{-1} and optimal OWI orientation would be ~0.39 rad. If this velocity turns out to be much lower, as the QES authors believed, then it would still be possible to measure the velocity of V_{Gal}, since the OWI sensitivity threshold is quite low.

Finally, given the OWI response, which is independent of whether the motion is circular or linear, it can be expected that it will be used to measure the linear velocity of the Earth's motion relative to the Cosmic Microwave Background (CMB) [11].

As is well known, CMB is the cooled thermal glow left over from the Big Bang. The temperature of the microwave background radiation is distributed unevenly

across the celestial sphere: in one direction, the background temperature is slightly higher than average, while in the opposite direction, it is lower. This characteristic structure, dividing the sky into two hemispheres, is called the microwave background dipole. Standard cosmology interprets the dipole as a kinematic effect caused by the solar system's motion relative to the microwave background at a velocity of approximately 370 km·s^{-1}, which causes a Doppler shift. The contribution to the phase shift $\Delta\psi$ at this linear motion velocity and optimal OWI orientation should be ~0.63 rad.

Determining the individual contribution of each velocity to the total phase shift $\Delta\psi$, determined by the vector sum of all the velocities of the Earth's motion (two circular and one linear), may prove to be a very complex task, but nevertheless a solvable problem, thanks to the ability to control the orientation of the axis direction and the scanning plane.

If the performance of the OWI is experimentally confirmed, this will allow us to determine other potential areas of its application in scientific and applied research and will become an important factor in clarifying the nature of the GSE itself, which is the subject of discussions among supporters of the standard Special Relativity and its alternatives.

4. Conclusions

This article discusses the OWI based on GSE for studying the rotational and uniform rectilinear motion of various objects.

To generate and isolate the phase shift of a wave carrying motion information, it is proposed to use scanning of a wave traveling along one arm of a two-beam interferometer. The design of this device and the calculation of the output signal are considered.

To test the OWI's functionality, an experiment has been proposed to measure the Earth's velocity around the Sun and, together with the Solar System, around the galactic center, as well as, hopefully, the Earth's translational velocity relative to the cosmic microwave background. If confirmed experimentally, the OWI will provide greater insight into the nature of the GSE and identify potential applications in scientific and applied research.

Conflicts of Interest

The author declares no conflicts of interest regarding the publication of this paper.

References

[1] Wang, R., Zheng, Y., Yao, A. and Langley, D. (2003) Modified Sagnac Experiment for Measuring Travel-Time Difference between Counter-Propagating Light Beams in a Uniformly Moving Fiber. *Physics Letters A*, **312**, 7-10. https://doi.org/10.1016/s0375-9601(03)00575-9

[2] Wang, R., Zheng, Y. and Yao, A. (2004) Generalized Sagnac Effect. *Physical Review Letters*, **93**, Article ID: 143901. https://doi.org/10.1103/physrevlett.93.143901

[3] Spavieri, G., Gillies, G.T. and Gaarder Haug, E. (2021) The Sagnac Effect and the Role

of Simultaneity in Relativity Theory. *Journal of Modern Optics*, **68**, 202-216. https://doi.org/10.1080/09500340.2021.1887384

[4] Choi, Y.-H. (2017) Theoretical Analysis of Generalized Sagnac Effect in the Standard Synchronization. *Canadian Journal of Physics*, **95**, 761-766. https://doi.org/10.1139/cjp-2016-0953

[5] Spavieri, G. and Haug, E.G. (2023) The One-Way Linear Effect, a First Order Optical Effect. *Heliyon*, **9**, e19590. https://doi.org/10.1016/j.heliyon.2023.e19590

[6] Sakharov, V.K. (2025) Interferometer Based on the Generalized Sagnac Effect. *Proceedings of the* 10*th All-Russian Dianov Conference on Fiber Optics*, Perm, 7-10 October 2025, 683-684.

[7] Römer, G.R.B.E. and Bechtold, P. (2014) Electro-Optic and Acousto-Optic Laser Beam Scanners. *Physics Procedia*, **56**, 29-39. https://doi.org/10.1016/j.phpro.2014.08.092

[8] Malykin, G.B. (2021) History of Development of the Methods and Interference Devices for Measuring a Small Optical Phase Difference (Review). *Optics and Spectroscopy*, **129**, 212-226. https://doi.org/10.1134/s0030400x21020090

[9] Malykin, G.B. and Pozdnyakova, V.I. (2020) Quadratic Sagnac Effect Recorded by an Observer in the Laboratory Frame. *Optics and Spectroscopy*, **128**, 1611-1617. https://doi.org/10.1134/s0030400x20100197

[10] Miller, D.C. (1933) The Ether-Drift Experiment and the Determination of the Absolute Motion of the Earth. *Reviews of Modern Physics*, **5**, 203-242. https://doi.org/10.1103/revmodphys.5.203

[11] Conklin, E.K. (1969) Velocity of the Earth with Respect to the Cosmic Background Radiation. *Nature*, **222**, 971-972. https://doi.org/10.1038/222971a0